

## Investigations on the Microstructure and Corrosion Performance of Different WC-based Cermet Coatings Deposited by High Velocity Oxy Fuel Process onto Magnesium Alloy Substrate

Ewa Jonda<sup>1\*</sup>, Leszek Łatka<sup>2</sup>, Artur Maciej<sup>3</sup>, Alexandr Khozhanov<sup>4</sup>

<sup>1</sup> Department of Engineering Materials and Biomaterials, Silesian University of Technology, ul. Konarskiego 18a, 44100 Gliwice, Poland

<sup>2</sup> Department of Metal Forming, Welding and Metrology, Faculty of Mechanical Engineering, Wrocław University of Science and Technology, ul. Łukasiewicza 5, 50371 Wrocław, Poland

<sup>3</sup> Department of Inorganic and Analytical Chemistry and Electrochemistry, Faculty of Chemistry, Silesian University of Technology, ul. Krzywoustego 6B, 44100 Gliwice, Poland

<sup>4</sup> School of IT&IS, D. Serikbayev East Kazakhstan Technical University, 69 Protozanov Street, 070004 Ust-Kamenogorsk, Kazakhstan

\* Corresponding author's e-mail: ewa.jonda@polsl.pl

### ABSTRACT

In the field of surface engineering, thermal spraying is very wide adopted in many branches of the industry. The main reasons of such situation are its flexibility as well as cost effectiveness. Among others, high velocity oxy fuel (HVOF) technique is dedicated for spraying hardmetal and cermet coatings, especially for wear- and corrosion resistance. Such type of coating could be a promising candidate as protective layer for magnesium alloys elements. These materials need a strong improvement in the corrosion protection as well as on the field of wear resistance in order to be widely used in the industry. In this work, different WC-based coatings, namely: (i) WC-Co, (ii) WC-Co-Cr and (iii) WC-Cr<sub>3</sub>C<sub>2</sub>-Ni manufactured by HVOF spraying, were investigated. The form of all feed-stock materials was agglomerated and sintered powder. All coatings were sprayed with the same technological parameters, especially spray distance which was equal to 400 mm on the AZ91 magnesium alloy substrate. The main aim of the studies was to investigate the influence of the powder material on the corrosion resistance of obtained coatings. The manufactured coatings were examined in terms of its microstructure, using scanning electron microscope (SEM) and corrosion performance, which was assessed in the electrochemical corrosion investigations in 3.5% NaCl solution by Tafel method. The study showed that the corrosion resistance increasing in such order: AZ91 < WC-Cr<sub>3</sub>C<sub>2</sub>-Ni < WC-Co < WC-Co-Cr. It should be stressed that WC-Cr<sub>3</sub>C<sub>2</sub>-Ni coating exhibits very low corrosion performance, which could be effected by relatively high porosity (c.a. 3 vol.%) and because of that the more complex composition promotes creation of many corrosion cells.

**Keywords:** AZ91 magnesium alloy, HVOF, thermal spraying, metal matrix composite coatings, microstructure, electrochemical corrosion.

### INTRODUCTION

New trends in the technological development is very closely related to the materials science. It could be a branch connected with new and original materials invention. On the other hand it could be a new applications of known materials. Among many engineering materials,

magnesium alloys are promising materials in the field of low-weight construction, due to very low density (c.a. 1.8 g·cm<sup>-3</sup>) and high specific strength [1, 2]. Its potential applications could be related to aerospace and automotive industry [3–5], electronic systems and even in medicine [6, 7]. Nevertheless, there are significant disadvantages of magnesium alloys, mostly connected with their

poor mechanical properties, wear and erosion resistance [8, 9]. However, the crucial drawback that prevents their widespread application is an impoverished corrosion performance [10, 11]. It was proved that magnesium acts as an anode and creates a galvanic cell with other metals [12, 13] what caused very low corrosion potential of Mg-based alloys. Moreover, besides galvanic corrosion, this material group is also easily exposed to transgranular and pitting corrosion [14, 15].

In order to improve such poor corrosion performance of the Mg-based alloys a different treatments could be used, as surface modification [16]. In the field of materials science it is also possible to improve by addition new elements, especially rare earth (RE) ones [17–19]. The potential of RE addition was proved and described e.g. in [20, 21]. Nevertheless, expected corrosion resistance could not meet the requirements of different branches of the industry, especially automotive or aviation ones. There are many methods of coatings manufacturing, which could be deposited on metallic substrates, including magnesium alloys, e.g.: anodization [22], electrodeposition [23], ionic liquid bath [24], micro arc oxidation [25], physical vapour deposition (PVD) [26, 27] and even conversion coatings [28]. Also thermal spraying methods could be used in order to manufacture coatings on magnesium alloys, as follow: cold spray [29], arc spray [30, 31], detonation-gun [32], flame spray [33] and plasma spray [34, 35]. As it was described in previous papers [36, 37], high velocity oxy fuel (HVOF) method is the most promising, especially for cermet coatings deposition. Although coatings sprayed on AZ31 alloy substrates are already well described [38], there is a gap in the literature related to the application of coatings on AZ91 alloy substrates.

In general, the HVOF method is widely used in order to obtain well-quality coatings which exhibit very good resistance against cyclic corrosion both, acetic acid salt spray and neutral salt spray from one hand and against electrochemical corrosion on the other hand [39–41]. One of the most frequently feedstock materials used for manufacturing corrosion resistance coating by HVOF process are cermet based on tungsten carbide (WC)

in cobalt or nickel matrix [42, 43]. However, there are only a few paper dedicated corrosion resistance coatings manufactured by HVOF method on the Mg-based alloys, even though the feedstock materials were aluminum based metal matrix composite [44] and 316L stainless steel [45].

The novelty of current paper was manufacturing of different WC-based cermet coatings on the Mg-based substrate. It was possible, like e.g. [46, 47], but this paper presents the comparison in comprehensive way in terms of corrosion resistance sprayed coatings. In present investigations all technological parameters, as well as feedstock powder delivery state were chosen in this way to make the comparison unaffected by other factors as much as possible. The functional properties of the coatings were tested in electrochemical corrosion environment which was 3.5% NaCl solution.

## MATERIALS AND METHODS

The substrate material was AZ91 magnesium alloy with chemical composition in Table 1. The dimensions were equal to 5 mm in the thickness and 100 mm in diameter. Before the spraying the surface of the substrate was sand-blasted by corundum grit F40 (according to the FEPA standard). The last stage of preparation was cleaning samples in the ultrasonic bath in the presence of ethanol.

The feedstock materials used in current studies were in the form of powder. Three commercially available powders were selected. The detailed information about these materials could be found in our previous paper [48]. The sample code and chemical composition of the coatings are collected in Table 2.

The cermet coatings were deposited by HVOF method (Fig. 1) with JP 5000 gun of TAFA system. As a fuel medium kerosene was used with flow rate equal to 26 l/h. Oxygen and nitrogen (transport gas) flow rate was equal to 900 l/min and 12 l/min, respectively. Powder was added with feed rate equal to 70 g/min, independently on material type.

The coatings' topography as well as its microstructure were observed by scanning electron

**Table 1.** Chemical composition of AZ91 magnesium alloy (according to ASTM B94 standard)

Chemical elements, wt%				
Al	Zn	Si	Mn	Mg
8.3–9.7	0.35–1.00	0.0–0.5	0.0–0.2	balance

**Table 2.** Sample code and chemical composition of coatings

Sample code	Chemical composition, wt%	Spray distance, mm
C1D3	WC-12Co	400
C2D3	WC-10Co-4Cr	
C3D3	WC-20Cr <sub>3</sub> C <sub>2</sub> -7Ni	

microscopy (SEM) on the top of samples and its cross-sections, respectively. The SEM was equipped with Energy Dispersive X-ray Spectrometer (EDS) analyzer in order to determine chemical composition.

The surface roughness in the as-sprayed state was determined by stylus profilometer, according to the ISO 4288 standard. The  $R_a$  parameter has been selected as a comparative and representative factor of coatings' surface roughness. For each sample five measurements were carried out and average, as well as standard deviation values were calculated.

The porosity of deposited coatings was assessed by image analysis according to the ASTM E2109–01 standard. The 20 images under the 1000x magnifications were taken into account in the open access software, ImageJ (1.50i version).

The corrosion resistance studies of the deposited AZ91 alloy were realized by the potentiodynamic Tafel method using an AUTOLAB PGSTAT100 potentiostat-galvanostat (Metrohm Autolab BV, The Netherlands). The investigation environment for corrosion tests was a 3.5% solution of NaCl at a temperature of 25°C. The surface area of the tested samples was 1 cm<sup>2</sup> which was limited by a rubber o-ring. The procedure was as follows: samples were stabilized for 3600 s at open circuit before the polarization and then open circuit potentials ( $E_{OCP}$ ) were determined. The potentiodynamic measurements (represented by linear sweep voltammetry – LSV) were carried at potentials values in the range from  $E_{OCP}-150$  mV

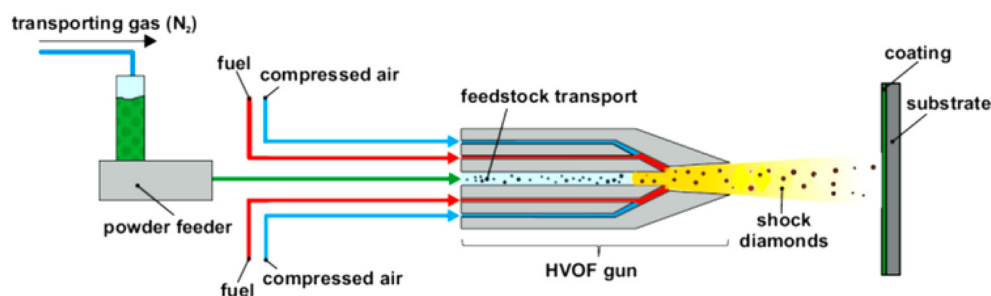
up to  $E_{OCP}+150$  mV with a scan rate equal to 0.167 mV·s<sup>-1</sup>. The obtained voltammograms were analyzed by NOVA 2.1. software, which was able to obtain corrosion properties of polarization resistance ( $R_p$ ), corrosion current density ( $j_{corr}$ ) and corrosion potential ( $E_{corr}$ ). Based on the corrosion current density the corrosion rate (CR) was calculated according to ASTM G102 standard. A double-walled (thermostatic) electrochemical cell with a three-electrode configuration was used. As the reference a saturated calomel electrode (SCE) was used, while as the counter electrode a platinum mesh was used. For comparison, analogical measurements were also conducted for not deposited AZ91 magnesium alloy. The surface structure of the tested samples after the polarization was analyzed by means of Hitachi TM 3000 scanning electron microscope.

## RESULTS

The SEM images of feedstock powders morphology (Fig. 2) confirmed its spherical shape what is very important from the facility of powders particles feeding. Moreover, all tested powders had very similar particles size and its distribution, which was important in the context of the comparison of deposits.

The topography of deposited samples confirmed a typical morphology of HVOF sprayed coatings (Fig. 3). The surface of the coatings is rather smooth, without craters or unexpected material peaks. Some irregularities could be observed are probably related to the carbide particles which exhibit high melting point and cannot be dissolved in the flame [50, 51].

In Table 3 the results of EDS determination of chemical composition (as an average from the area equal to c.a. 20,000 μm<sup>2</sup>) of deposited coatings are collected. The average values of surface roughness expressed by  $R_a$  parameter are: 4.39

**Fig. 1.** Scheme of HVOF spraying method used in current studies [49]

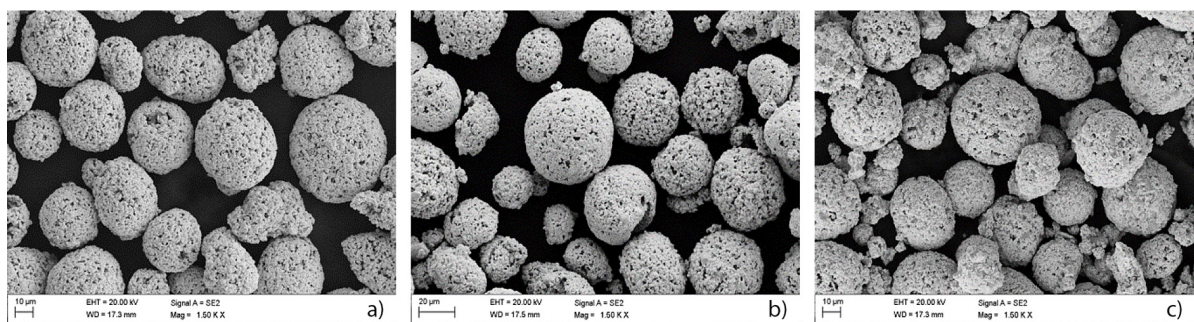


**Fig. 2.** Morphology of the feedstock powders: WC-12Co (a), WC-10Co-4Cr (b), WC-20Cr<sub>3</sub>C<sub>2</sub>-7Ni (c)



**Fig. 3.** The surface topography of the sprayed coatings: C1D3 (a), C2D3 (b), C3D3 (c)

$\pm 0.45 \mu\text{m}$ ,  $4.97 \pm 0.24 \mu\text{m}$  and  $5.40 \pm 0.34 \mu\text{m}$  for C1D3, C2D3 and C3D3, respectively. Such roughness values are in good agreement with the literature [52].

The SEM observations of the coatings' microstructure at lower magnification (Fig. 4) confirmed that all samples exhibit compact and dense structure, as could be found for the same coatings type deposited by HVOF on steel substrates [53, 54]. The average thickness of the coatings was in the range from 160 up to 200  $\mu\text{m}$ .

The detailed microscopy observations at higher magnification (Fig. 5) also confirmed dense structure, which could be found in literature [55]. Nevertheless, there are some cracks, which could result from thermal stresses occurring during deposition process [56]. Other cause of the cracks and small pores presence could be a short residence time in the flame of the powder particles and resulting relatively poor heat treatment [57].

The porosity assessment results revealed that with HVOF method it is possible to obtain relatively dense coatings, especially at the investigated

spray distance (400 mm). Obtained porosity values are as follow:  $2.9 \pm 0.6\%$ ,  $2.2 \pm 0.5\%$  and  $3.0 \pm 0.5\%$  for C1D3, C2D3 and C3D3, respectively. Such porosity level is in good agreement with the literature [58, 59].

On the basis of the conducted corrosion studies the beneficial influence of the HVOF sprayed coatings on the corrosion resistance of the magnesium-based substrate was observed. For all types of cermet coatings it were found higher values of polarization resistance ( $R_p$ ), as well as lower values of corrosion current density ( $j_{corr}$ ) in the comparison to the uncoated AZ91 which was taken as a reference. All the results are collected in Table 4. The corrosion resistance of the AZ91 alloy was slightly outstanding but the obtained results of the potentiodynamic measurements were relatively similar to the reported in literature [60,61]. Besides reported corrosion rates of cermet coatings (Table 4) have higher values than those signalled for bare metal alloys such as stainless steel, which could be used as reference [62].

**Table 3.** Chemical composition of sprayed coatings, determined by EDS

Sample	Chemical composition, wt%				
	W	C	Co	Cr	Ni
C1D3	78.5	3.0	18.5	–	–
C2D3	72.2	3.3	18.0	6.5	–
C3D3	64.4	3.8	–	22.3	9.5

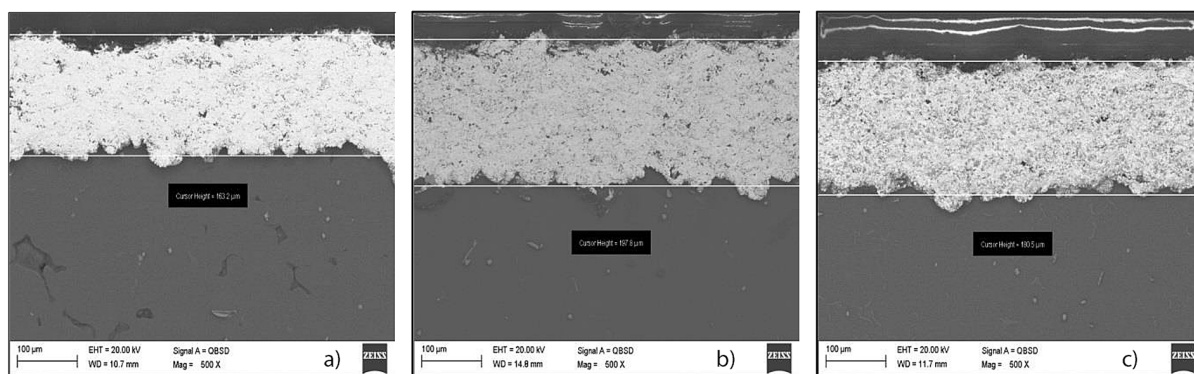


Fig. 4. The SEM images of coatings' cross sections: C1D3 (a), C2D3 (b), C3D3 (c)

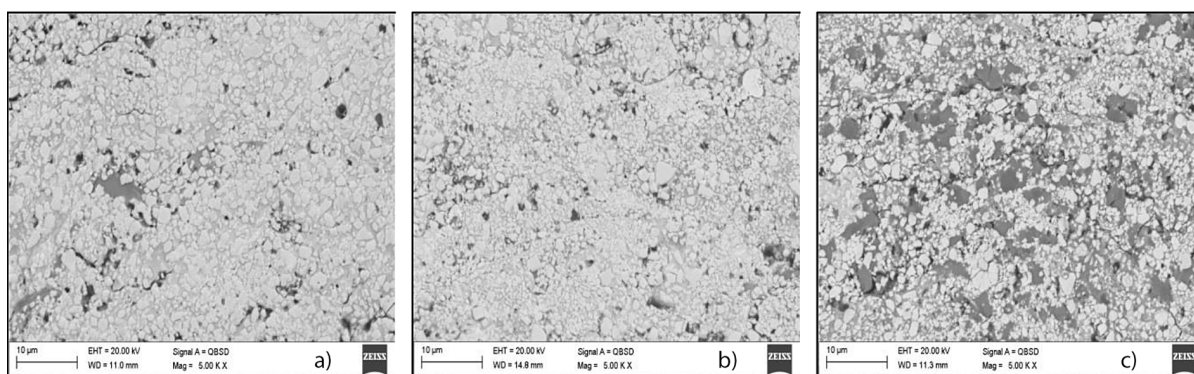


Fig. 5. The SEM images detailed microstructures of samples: C1D3 (a), C2D3 (b), C3D3 (c)

After corrosion test the obtained results for corrosion potential ( $E_{corr}$ ) of the sprayed samples were shifted towards more positive values than the reference AZ91 one. A typical values of the  $E_{corr}$  for AZ91 in chloride solutions are in the range from  $-1.60$  up to  $-1.50$  V [63,64]. For all the coatings higher values of  $E_{corr}$  are observed (Table 4). It shows the cathodic nature of the deposited coatings and could be related to the some discontinuities (e.g. porosity). In such corrosion cell, the magnesium substrate becomes an anode and starts to corrode. From corrosion prevent it is a fundamental issue, because requirements for such coatings (as tightness and compactness). Otherwise the corrosion rate of such defected coating will be even higher than uncoated AZ91 alloy. This phenomenon was described in [46] during neutral salt spray tests carried out on HVOF

sprayed coatings. As it could be seen in Table 4 and Fig. 6,  $E_{corr}$  and  $R_p$  values for C3D3 sample are relatively close to the AZ91 substrate. It could be explained by the highest porosity of this coating. Moreover, the more complex chemical composition promotes the formation of more corrosion cells [65]. The sample was also characterized by the highest roughness which influences on the improvement of the real tested area which is also important here. There are much more number of corrosion cells on the more expanded surface in comparison to a smoother surface. On the other hand, two others samples are characterized by much better corrosion resistance. The good corrosion resistance of the C1D3 sample may be explained by its relatively simple composition (just two components, without nickel) which limits the corrosion cells formation. The best performance

Table 4. The results of the potentiodynamic measurements in 3.5% NaCl solution

Sample	$j_{corr}$ , $\mu A \cdot cm^{-2}$	$R_p$ , $\Omega \cdot cm^2$	$E_{corr}$ , V	CR, $mm \cdot yr^{-2}$
AZ91	1612.1±265,3	17.8±2.9	- 1.559±0.019	34.52±5.68
C1D3	59.1±8.7	432.5±63.5	- 0.978±0.011	1.27±0.19
C2D3	14.3±2.0	2621.1±358.8	- 0.697±0.016	0.31±0.04
C3D3	1249.0±155.3	24.9±3.1	- 1.230±0.014	26.74±3.32

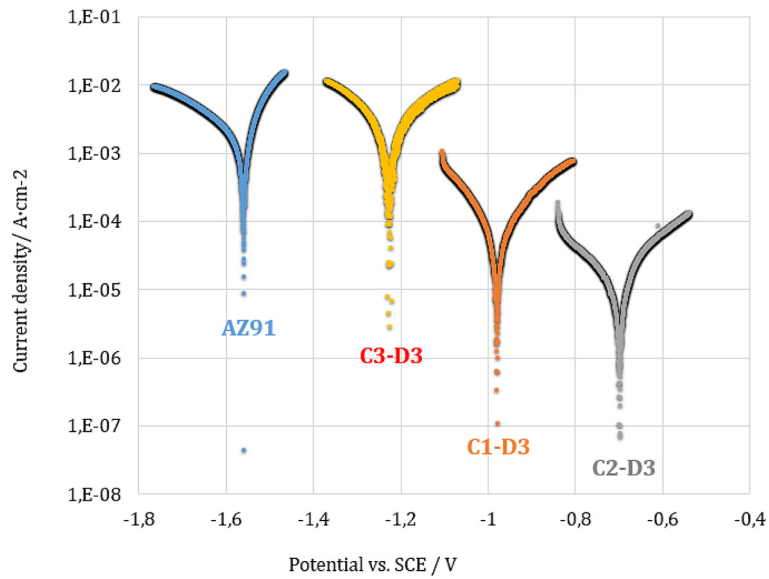


Fig. 6. Potentiodynamic curves for the tested samples

is exhibited by C2D3 coating, because of presence of Cr addition. Chromium is a metal which may easily transform to passive state so the property make the WC-Co-Cr coating the best among the studied ones. The  $R_p$  and  $j_{corr}$  values for C2D3 sample were c.a. 150 and 115 times better, respectively than for AZ91 reference sample.

The courses of the OCP curves (Fig.7) provided additional, interesting information about the stability of the tested samples immersed in the 3.5% NaCl solution. In the case of the well-resistant coatings (C2D3 and C1D3), the OCP was very stable throughout one hour of the immersion which confirms their good tightness and no influence of the magnesium alloy substrate. The open

circuit potential of the significantly worse coating (C3D3) was practically stable for about 1700 s and has been staying on a relatively high level of the potential (about -0.9 V vs. SCE). After this time the OCP began to drop drastically, finally reaching a value of less than -1.2 V. The observed fast falling of OCP towards the value of  $E_{OCP}$  of magnesium alloy substrate indicates a soaking of the WC-Cr<sub>3</sub>C<sub>2</sub>-Ni coating by the corrosive medium resulting from its poor tightness (and the highest porosity). As a result, relatively strong corrosion cells could have formed, especially in the area of the coating/substrate interface. Apart from the complexity of the chemical composition of the C3D3 HVOF coating, the penetration of

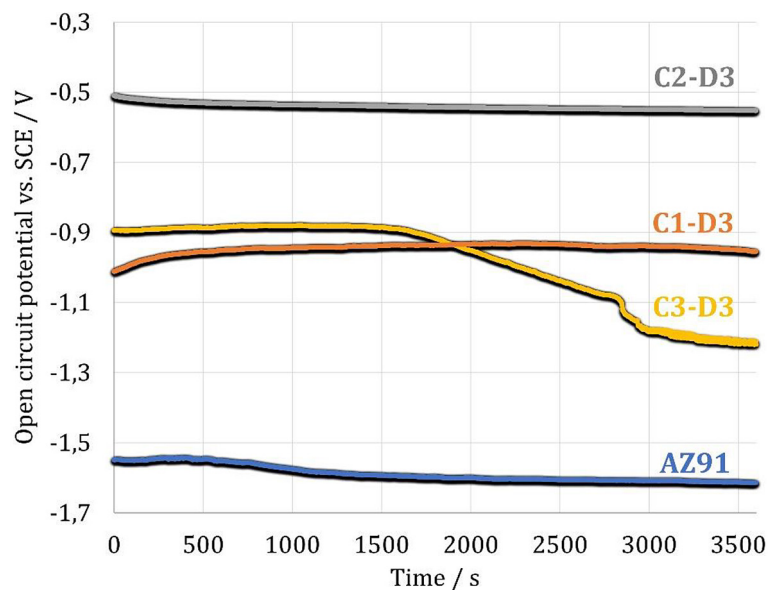


Fig. 7. The open circuit potential curves for the tested samples

the solution clearly explains its weak corrosion resistance.

The degree of corrosion resistance of the HVOF coatings was also confirmed by microscopic analysis of surface structure after the potentiodynamic measurements (Fig. 8). The structure of the samples C1D3 and C2D3 are practically unchanged in comparison to their appearance

before the polarization which proved their high corrosion resistance in the aggressive chloride solution. In the case of the C3D3 sample the surface of tested area was covered by white-gray corrosion products of magnesium alloy substrate. The layer of corrosion products was characterized by porous and well-expanded structure which was very similar to structure of corrosion products of

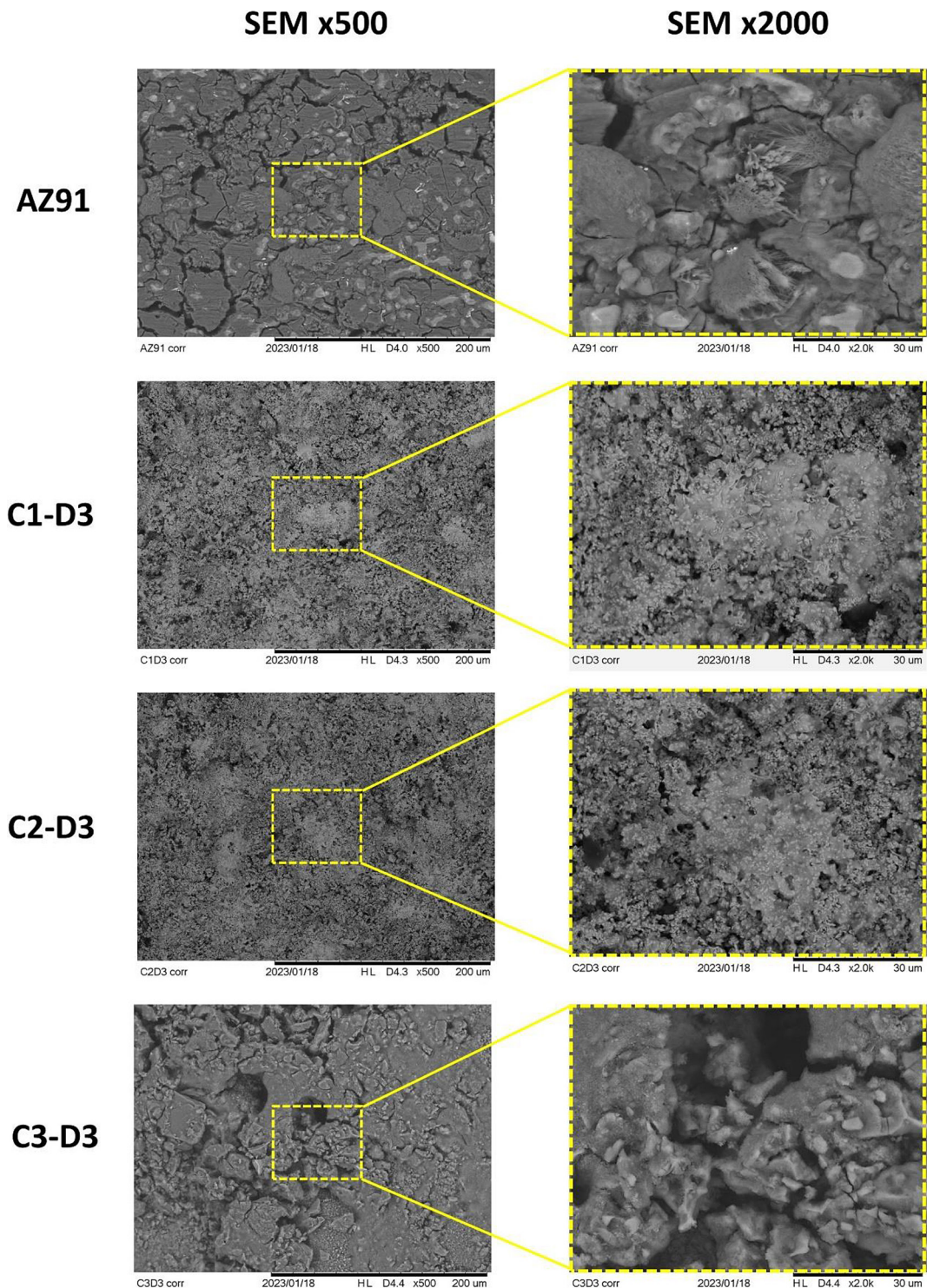


Fig. 8. The SEM images of the surface structure of coatings after the potentiodynamic tests

AZ91 sample. The remains of HVOF coatings were not observed in the test area. The WC-based coating was degrading by intensive hydrogen evolution during the anodic polarization and the remains were on the bottom of corrosion cell.

## CONCLUSIONS

Based on the tests carried out on the different cermet coatings deposited on the AZ91 magnesium alloy substrate with high velocity oxy fuel (HVOF) spraying, the following conclusions could be made. The interface between coating and substrate was clear, no evidence of delamination or other discontinuities was observed. The coating adheres tightly to the substrate and fills all surface irregularities. Microscopic investigation revealed that there are some voids and cracks, which could promote porosity and small quantity of partially melted initial powder particles which was especially observed for WC-Cr<sub>3</sub>C<sub>2</sub>-Ni coating where porosity was equal to 3.0 ± 0.5 vol.%. The surface roughness of the sprayed coatings was greater than the roughness of the AZ91 magnesium alloy substrate ( $R_a = 0.4 \pm 0.15 \mu\text{m}$ ) especially in the case of double carbide coating C3D3 ( $R_a = 5.40 \pm 0.34 \mu\text{m}$ ). The porosity values are relatively high, as for HVOF sprayed coatings, nevertheless it is connected with high spray distance (400 mm) which was selected in order to prevent magnesium alloy against the flame. The best corrosion resistance is exhibited by C2D3 coating. Also, good resistance was characteristic for C1D3 coating. In case of C3D3 coating the corrosion resistance was similar like uncoated AZ91 substrate. It could be because of relatively high porosity of the C3-D3 coating.

## Acknowledgments

Author gratefully acknowledges Resurs Company in Warszawa (Poland) for help in the coatings deposition process.

This research was financed by the pro-quality grant of the President Silesian University of Technology, no. 10/010/RGJ22/1084.

## REFERENCES

1. Friedrich H.E., Mordike B.L., eds. Magnesium technology: metallurgy, design data, applications, Springer, Berlin; New York, 2006.

2. Tan J., Ramakrishna S. Applications of Magnesium and Its Alloys: A Review. *Applied Sciences* 2021; 11: 6861. <https://doi.org/10.3390/app11156861>
3. Furuya H., Kogiso N., Matunaga S., Senda K. Applications of Magnesium Alloys for Aerospace Structure Systems. *MSF* 2000; 350–351: 341–348. <https://doi.org/10.4028/www.scientific.net/MSF.350-351.341>
4. Joost W.J., Krajewski P.E. Towards magnesium alloys for high-volume automotive applications. *Scripta Materialia* 2017; 128: 107–112. <https://doi.org/10.1016/j.scriptamat.2016.07.035>
5. Dziubińska A., Gontarz A., Dziubiński M., Barszcz M. The forming of magnesium alloy forgings for aircraft and automotive applications. *Adv. Sci. Technol. Res. J.* 2016; 10: 158–168. <https://doi.org/10.12913/22998624/64003>
6. Yang Y., Xiong X., Chen J., Peng X., Chen D., Pan F. Research advances in magnesium and magnesium alloys worldwide in 2020. *Journal of Magnesium and Alloys* 2021; 9: 705–747. <https://doi.org/10.1016/j.jma.2021.04.001>
7. Li N., Zheng Y. Novel Magnesium Alloys Developed for Biomedical Application: A Review. *Journal of Materials Science & Technology* 2013; 29: 489–502. <https://doi.org/10.1016/j.jmst.2013.02.005>
8. Iwaszko J., Kudła K. Microstructure, hardness, and wear resistance of AZ91 magnesium alloy produced by friction stir processing with air-cooling. *Int J Adv Manuf Technol.* 2021; 116: 1309–1323. <https://doi.org/10.1007/s00170-021-07474-9>
9. Kondaiah V.V., Pavanteja P., Afzal Khan P., Anand Kumar S., Dumpala R., Ratna Sunil B. Microstructure, hardness and wear behavior of AZ31 Mg alloy – fly ash composites produced by friction stir processing. *Materials Today: Proceedings* 2017; 4: 6671–6677. <https://doi.org/10.1016/j.matpr.2017.06.441>
10. Song G.L., Atrens A. Corrosion Mechanisms of Magnesium Alloys. *Adv. Eng. Mater.* 1999; 1: 11–33. [https://doi.org/10.1002/\(SICI\)1527-2648\(199909\)1:1<11::AID-ADEM11>3.0.CO;2-N](https://doi.org/10.1002/(SICI)1527-2648(199909)1:1<11::AID-ADEM11>3.0.CO;2-N)
11. Pardo A., Merino M.C., Coy A.E., Viejo F., Arabal R., Feliú S. Influence of microstructure and composition on the corrosion behaviour of Mg/Al alloys in chloride media. *Electrochimica Acta* 2008; 53: 7890–7902. <https://doi.org/10.1016/j.electacta.2008.06.001>
12. Song G.-L., Xu Z. The surface, microstructure and corrosion of magnesium alloy AZ31 sheet. *Electrochimica Acta* 2010; 55: 4148–4161. <https://doi.org/10.1016/j.electacta.2010.02.068>
13. Zhang L., Yang S., Lv X., Jie X. Wear and Corrosion Resistance of Cold-Sprayed Cu-Based Composite Coatings on Magnesium Substrate. *J Therm*

- Spray Tech. 2019; 28: 1212–1224. <https://doi.org/10.1007/s11666-019-00887-9>
14. Guo K.W. A Review of Magnesium/Magnesium Alloys Corrosion and its Protection. *Recent Pat. Corros. Sci.* 2010; 2: 13–21. <https://doi.org/10.2174/1877610801002010013>
  15. Radha R., Sreekanth D. Insight of magnesium alloys and composites for orthopedic implant applications – a review. *Journal of Magnesium and Alloys* 2017; 5: 286–312. <https://doi.org/10.1016/j.jma.2017.08.003>
  16. Luan B.L., Gray J., Yang L.X., Cheong W.J., Shoosmith D. Surface Modification of AZ91 Magnesium Alloy, *MSF* 2007; 546–549: 513–518. <https://doi.org/10.4028/www.scientific.net/MSF.546-549.513>
  17. Sivashanmugam N., Harikrishna K.L. Influence of Rare Earth Elements in Magnesium Alloy – A Mini Review. *MSF* 2020; 979: 162–166. <https://doi.org/10.4028/www.scientific.net/MSF.979.162>
  18. Calado L.M., Carnezim M.J., Montemor M.F. Rare Earth Based Magnesium Alloys—A Review on WE Series, *Front. Mater.* 2022; 8: 804906. <https://doi.org/10.3389/fmats.2021.804906>
  19. Liu D., Yang D., Li X., Hu S. Mechanical properties, corrosion resistance and biocompatibilities of degradable Mg-RE alloys: A review. *Journal of Materials Research and Technology* 2019; 8: 1538–1549. <https://doi.org/10.1016/j.jmrt.2018.08.003>
  20. Azzeddine H., Hanna A., Dakhouché A., Rabahi L., Scharnagl N., Dopita M., Brisset F., Helbert A.-L., Baudin T. Impact of rare-earth elements on the corrosion performance of binary magnesium alloys. *Journal of Alloys and Compounds* 2020; 829: 154569. <https://doi.org/10.1016/j.jallcom.2020.154569>
  21. Meng J., Sun W., Tian Z., Qiu X., Zhang D. Corrosion performance of magnesium (Mg) alloys containing rare-earth (RE) elements, in: *Corrosion Prevention of Magnesium Alloys*. Elsevier, 2013; 38–60. <https://doi.org/10.1533/9780857098962.1.38>
  22. Zhang R.F., Shan D.Y., Han E.H. Two-Step Anodization of AZ91 Magnesium Alloy. *MSF* 2005; 488–489: 653–656. <https://doi.org/10.4028/www.scientific.net/MSF.488-489.653>
  23. Singh C., Tiwari S.K., Singh R. Exploring environment friendly nickel electrodeposition on AZ91 magnesium alloy: Effect of prior surface treatments and temperature of the bath on corrosion behaviour. *Corrosion Science* 2019; 151: 1–19. <https://doi.org/10.1016/j.corsci.2019.02.004>
  24. Singh C., Tiwari S.K., Singh R. Development of corrosion-resistant electroplating on AZ91 Mg alloy by employing air and water-stable eutectic based ionic liquid bath. *Surface and Coatings Technology* 2021; 428: 127881. <https://doi.org/10.1016/j.surfcoat.2021.127881>
  25. Veys-Renaux D., Barchiche C.-E., Rocca E. Corrosion behavior of AZ91 Mg alloy anodized by low-energy micro-arc oxidation: Effect of aluminates and silicates. *Surface and Coatings Technology* 2014; 251: 232–238. <https://doi.org/10.1016/j.surfcoat.2014.04.031>
  26. Hoche H., Rosenkranz C., Delp A., Lohrengel M.M., Broszeit E., Berger C. Investigation of the macroscopic and microscopic electrochemical corrosion behaviour of PVD-coated magnesium die cast alloy AZ91. *Surface and Coatings Technology* 2005; 193: 178–184. <https://doi.org/10.1016/j.surfcoat.2004.08.204>
  27. Dybowski K., Januszewicz B., Kowalczyk P., Batory D. Hybrid layer type Cr/LPC. *Adv. Sci. Technol. Res. J.* 2017; 11: 23–27. <https://doi.org/10.12913/22998624/67672>
  28. Ardelean H., Frateur I., Marcus P. Corrosion protection of magnesium alloys by cerium, zirconium and niobium-based conversion coatings. *Corrosion Science* 2008; 50: 1907–1918. <https://doi.org/10.1016/j.corsci.2008.03.015>
  29. Wang Q., Spencer K., Birbilis N., Zhang M.-X. The influence of ceramic particles on bond strength of cold spray composite coatings on AZ91 alloy substrate. *Surface and Coatings Technology* 2010; 205: 50–56. <https://doi.org/10.1016/j.surfcoat.2010.06.008>
  30. Catar R., Altun H. Improvement of corrosion and stress corrosion properties of magnesium alloys by coating aluminum with the electric arc spray method. *Materials & Corrosion* 2022; 73: 1766–1775. <https://doi.org/10.1002/maco.202213156>
  31. Majewski D., Hejwowski T., Łukasik D. The Influence of Microstructure of Arc Sprayed Coatings on Wear Resistance. *Adv. Sci. Technol. Res. J.* 2018; 12: 285–292. <https://doi.org/10.12913/22998624/86210>
  32. Kumar S., Kumar A., Kumar D., Jain J. Thermally sprayed alumina and ceria-doped-alumina coatings on AZ91 Mg alloy, *Surface and Coatings Technology* 2017; 332: 533–541. <https://doi.org/10.1016/j.surfcoat.2017.05.096>
  33. Gao P.H., Li J.P., Yang Z., Guo Y.C., Wang Y.R. Corrosion Resistance of Al-12Si Coatings on AZ91 Magnesium Alloy Prepared through Flame Spray. *MSF* 2013; 765: 639–643. <https://doi.org/10.4028/www.scientific.net/MSF.765.639>
  34. Kubatík T.F., Pala Z., Neufuss K., Vilémová M., Mušálek R., Stoužil J., Slepíčka P., Chráska T. Metallurgical bond between magnesium AZ91 alloy and aluminium plasma sprayed coatings. *Surface and Coatings Technology* 2015; 282: 163–170. <https://doi.org/10.1016/j.surfcoat.2015.10.032>
  35. Pashechko M., Kindrachuk M., Gumeniuk I., Tisov O., Zahrebelniy V. Functional Plasma-Deposited

- Coatings. *Adv. Sci. Technol. Res. J.* 2017; 11: 301–304. <https://doi.org/10.12913/22998624/80996>
36. Jonda E., Łatka L., Tomiczek A., Godzierz M., Pakieła W., Nuckowski P. Microstructure Investigation of WC-Based Coatings Prepared by HVOF onto AZ31 Substrate. *Materials* 2021; 15: 40. <https://doi.org/10.3390/ma15010040>.
  37. Jonda E., Łatka L. Comparative Analysis of Mechanical Properties of WC-based Cermet Coatings Sprayed by HVOF onto AZ31 Magnesium Alloy Substrates. *Adv. Sci. Technol. Res. J.* 2021; 15: 57–64. <https://doi.org/10.12913/22998624/135979>
  38. Morelli S., Rombolà G., Bolelli G., Lopresti M., Puddu P., Boccaleri E., Seralessandri L., Palin L., Testa V., Milanese M., Lusvarghi L. Hard ultralight systems by thermal spray deposition of WC-CoCr onto AZ31 magnesium alloy. *Surface and Coatings Technology* 2022; 451: 129056. <https://doi.org/10.1016/j.surfcoat.2022.129056>
  39. Lyphout C., Sato K., Houdkova S., Smazalova E., Lusvarghi L., Bolelli G., Sassatelli P. Tribological Properties of Hard Metal Coatings Sprayed by High-Velocity Air Fuel Process. *J Therm Spray Tech.* 2016; 25: 331–345. <https://doi.org/10.1007/s11666-015-0285-4>
  40. Wood R.J.K., Herd S., Thakare M.R. A critical review of the tribocorrosion of cemented and thermal sprayed tungsten carbide. *Tribology International* 2018; 119: 491–509. <https://doi.org/10.1016/j.triboint.2017.10.006>
  41. Ahmed R., Vourlias G., Algoburi A., Vogiatzis C., Chaliampalias D., Skolianos S., Berger L.-M., Paul S., Faisal N.H., Toma F.-L., Al-Anazi N.M., Goosen M.F.A. Comparative Study of Corrosion Performance of HVOF-Sprayed Coatings Produced Using Conventional and Suspension WC-Co Feedstock. *J Therm Spray Tech.* 2018; 27: 1579–1593. <https://doi.org/10.1007/s11666-018-0775-2>
  42. Souza V.A.D., Ne A. Linking electrochemical corrosion behaviour and corrosion mechanisms of thermal spray cermet coatings (WC<sub>A</sub>/CrNi and WC/ CrC<sub>A</sub>/CoCr). *Materials Science and Engineering A.* 2003.
  43. Bolelli G., Giovanardi R., Lusvarghi L., Manfredini T. Corrosion resistance of HVOF-sprayed coatings for hard chrome replacement. *Corrosion Science* 2006; 48: 3375–3397. <https://doi.org/10.1016/j.corsci.2006.03.001>.
  44. Taltavull C., Lopez A.J., Torres B., Atrens A., Rams J. Optimisation of the high velocity oxygen fuel (HVOF) parameters to produce effective corrosion control coatings on AZ91 magnesium alloy: Optimisation of the high velocity oxygen fuel (HVOF) parameters. *Materials and Corrosion* 2015; 66423–66433. <https://doi.org/10.1002/maco.201407982>
  45. García-Rodríguez S., López A.J., Torres B., Rams J. 316L stainless steel coatings on ZE41 magnesium alloy using HVOF thermal spray for corrosion protection. *Surface and Coatings Technology* 2016; 287: 9–19. <https://doi.org/10.1016/j.surfcoat.2015.12.075>
  46. Parco M., Zhao L., Zwick J., Bobzin K., Lugscheider E. Investigation of HVOF spraying on magnesium alloys. *Surface and Coatings Technology* 2006; 201: 3269–3274. <https://doi.org/10.1016/j.surfcoat.2006.06.047>
  47. Buchtík M., Másilko J., Vyklický O., Filipenský J., Wasserbauer J., Ptáček P. Microstructural characterization and wear behavior of WC-CoCr coating on AZ91 magnesium alloy 2019; 922–927. <https://doi.org/10.37904/metal.2019.730>
  48. Jonda E., Szala M., Sroka M., Łatka L., Walczak M. Investigations of cavitation erosion and wear resistance of cermet coatings manufactured by HVOF spraying. *Applied Surface Science* 2023; 608: 155071. <https://doi.org/10.1016/j.apusc.2022.155071>
  49. Łatka L., Pawłowski L., Winnicki M., Sokołowski P., Małachowska A., Kozerski S. Review of Functionally Graded Thermal Sprayed Coatings. *Applied Sciences* 2020; 10: 5153. <https://doi.org/10.3390/app10155153>
  50. Agüero A., Camón F., García de Blas J., del Hoyo J.C., Muelas R., Santaballa A., Ulargui S., Vallés P. HVOF-Deposited WCCoCr as Replacement for Hard Cr in Landing Gear Actuators. *J Therm Spray Tech.* 2011; 20: 1292–1309. <https://doi.org/10.1007/s11666-011-9686-1>
  51. Ding X., Ke D., Yuan C., Ding Z., Cheng X. Microstructure and Cavitation Erosion Resistance of HVOF Deposited WC-Co Coatings with Different Sized WC, *Coatings.* 2018; 8: 307. <https://doi.org/10.3390/coatings8090307>
  52. Șerban V.A., Uțu I.D., Mărginean G. Substrate influence on the properties of thermally sprayed WC–Cr–Ni cermet coatings, *J. Optoelectron. Adv. Mater.* 2015; 17: 1425–1430.
  53. Wang H., Qiu Q., Gee M., Hou C., Liu X., Song X. Wear resistance enhancement of HVOF-sprayed WC-Co coating by complete densification of starting powder. *Materials & Design* 2020; 191: 108586. <https://doi.org/10.1016/j.matdes.2020.108586>
  54. Song B., Murray J.W., Wellman R.G., Pala Z., Hussain T. Dry sliding wear behaviour of HVOF thermal sprayed WC-Co-Cr and WC-CrxCy-Ni coatings. *Wear* 2020; 442–443: 203114. <https://doi.org/10.1016/j.wear.2019.203114>
  55. Hong S., Wu Y.P., Gao W.W., Wang B., Guo W.M., Lin J.R. Microstructural characterisation and microhardness distribution of HVOF sprayed WC–10Co–4Cr coating. *Surface Engineering* 2014; 30: 53–58. <https://doi.org/10.1179/1743294413Y.0000000184>

56. Zhang H., Chen X., Gong Y., Tian Y., McDonald A., Li H. In-situ SEM observations of ultrasonic cavitation erosion behavior of HVOF-sprayed coatings. *Ultrasonics Sonochemistry* 2020; 60: 104760. <https://doi.org/10.1016/j.ultsonch.2019.104760>
57. Yao H.-L., Yang C., Yi D.-L., Zhang M.-X., Wang H.-T., Chen Q.-Y., Bai X.-B., Ji G.-C. Microstructure and mechanical property of high velocity oxy-fuel sprayed WC-Cr<sub>3</sub>C<sub>2</sub>-Ni coatings. *Surface and Coatings Technology* 2020; 397: 126010. <https://doi.org/10.1016/j.surfcoat.2020.126010>
58. Murugan K., Ragupathy A., Balasubramanian V., Sridhar K. Optimizing HVOF spray process parameters to attain minimum porosity and maximum hardness in WC-10Co-4Cr coatings. *Surface and Coatings Technology* 2014; 24790–102. <https://doi.org/10.1016/j.surfcoat.2014.03.022>
59. Zhang S.-H., Cho T.-Y., Yoon J.-H., Li M.-X., Shum P.W., Kwon S.-C. Investigation on microstructure, surface properties and anti-wear performance of HVOF sprayed WC-CrC-Ni coatings modified by laser heat treatment. *Materials Science and Engineering: B*. 2009; 162: 127–134. <https://doi.org/10.1016/j.mseb.2009.03.017>
60. Al Bacha S., Aubert I., Zakhour M., Nakhl M., Bobet J.L. Valorization of AZ91 by the hydrolysis reaction for hydrogen production (Electrochemical approach). *Journal of Magnesium and Alloys* 2021; 9: 1942–1953. <https://doi.org/10.1016/j.jma.2020.12.007>
61. Zhang Y., Shen X. Facile fabrication of robust superhydrophobic coating for enhanced corrosion protection on AZ91 magnesium alloy by electroless Ni-B/GO plating. *Surface and Coatings Technology* 2023; 455: 129213. <https://doi.org/10.1016/j.surfcoat.2022.129213>
62. Walczak M., Szala M., Okuniewski W. Assessment of Corrosion Resistance and Hardness of Shot Peened X5CrNi18–10 Steel. *Materials* 2022; 15: 9000. <https://doi.org/10.3390/ma15249000>
63. Wu P., Zhang Z., Xu F., Deng K., Nie K., Gao R. Effect of duty cycle on preparation and corrosion behavior of electrodeposited calcium phosphate coatings on AZ91. *Applied Surface Science* 2017; 426: 418–426. <https://doi.org/10.1016/j.apusc.2017.07.111>
64. Wang B., Liu X., Wang Y., Ding J., Wei S., Xia X., Liu M., Xu B. Microstructure and anti-corrosion properties of supersonic plasma sprayed Al-coating with Nano-Ti polymer sealing on AZ91-Magnesium alloy. *Journal of Materials Research and Technology* 2022; 21: 2730–2742. <https://doi.org/10.1016/j.jmrt.2022.10.086>
65. Calderon S., Alves C.F.A., Manninen N.K., Cavaleiro A., Carvalho S. Electrochemical Corrosion of Nano-Structured Magnetron-Sputtered Coatings. *Coatings* 2019; 9: 682. <https://doi.org/10.3390/coatings9100682>